Proc. Nat. Acad. Sci. USA
Vol. 71, No. 5, pp. 1618–1622, May 1974

Quantitative Analysis of Mass and Energy Balance in Non-Ideal Models of the Renal Counterflow System*

(concentration of urine/kidney tubule/vasa recta/central core model/urea)

JOHN L. STEPHENSON†, R. P. TEWARSON‡, AND RAYMOND MEJIA†

† Section on Theoretical Biophysics, NHLI, and Mathematical Research Branch, NIAMDD, NIH, Bethesda, Maryland 20014; and
‡ Department of Applied Mathematics and Statistics, State University of New York, Stony Brook, N.Y. 11790

Communicated by Robert W. Berliner, January 21, 1974

ABSTRACT **A modified Newton-Raphson method for solving finite difference equations for the renal counterflow system is described. The method has proved generally stable and efficient, and has given significant computational results for a variety of models: calculations on single solute models of the coupled vasa recta nephron counterflow system have shown that for large water and solute permeabilities of the exchanging membranes, behavior of the non-ideal system approaches that of the previously described ideal central core model. Concentration by salt and urea mixing in two solute models has been analyzed and previous conclusions from central core models have been found to remain valid in non-ideal systems. The numerical solutions have set some order of magnitude bounds on permeability requirements for concentration in different types of non-ideal systems. Finally, from the detailed concentration profiles it has been possible to relate the rate of free energy creation and dissipation from transmembrane transport of solutes and water to the net rate of free energy efflux from the counterflow system, and so to compute in a given model the fraction of power used for solute concentration.**

It has been proposed in previous papers (1–3) that the behavior of the intricately coupled nephrovascular counterflow system of the renal medulla (4) approaches as a limiting case that of a four-tube model: the vascular counterflow exchanger is represented by a single tube—the central core, closed at the papillary end and open at the corticomedullary junction—which exchanges with three other tubes corresponding respectively to ascending Henle's limb (AHL), descending Henle's limb (DHL), and collecting duct (CD). Under the assumption that total solute concentrations in core, DHL, and CD are nearly the same at each level of the medulla, it has been possible to develop an approximate analytic theory of the ideal central core concentrating engine and so of the medullary counterflow system. This assumption implies very high solute and water permeability of the vasa recta and very high osmotic water permeability and (or) solute permeability of DHL and CD. The behavior of non-ideal models with finite permeabilities will deviate from that of the ideal central core model. In general, the differential equations describing non-ideal models must be solved numerically. For certain single-solute models this has been done by converting the two-point boundary value problem to an initial value problem (5), but this method tends to be unstable, requiring very good initial estimates to converge, and does not extend readily to two-solute models.

Abbreviations: AHL, ascending Henle's limb; DHL, descending Henle's limb; CD, collecting duct; DVR, descending vasa recta; AVR, ascending vasa recta; DN, distal cortical nephron.

* A preliminary report of this work was given in ref. 13.

In this paper we outline a modified Newton–Raphson method for solving globally finite difference equations approximating the differential equations. The method has proved generally applicable to a variety of models of the renal counterflow system. In this paper we summarize some significant preliminary computational results. Detailed descriptions of both the method and the results are in preparation.

Solution of finite difference equations

Under suitable restrictions the steady state differential equations for the renal counterflow system are (2, 6):

$$dF_{ik}/dx = -J_{ik}, \quad [1]$$

$$dF_{iv}/dx = -J_{iv}, \quad [2]$$

$$J_{ik} = \Sigma_p J_{ip,k}, \quad [3]$$

$$J_{iv} = \Sigma_p J_{ip,v}, \quad [4]$$

$$F_{ik} = F_{iv}c_{ik}, \text{ and} \quad [5]$$

$$dP_i/dx = -R_{iF}F_{iv}, \quad [6]$$

where F_{ik} is the axial flow of the kth solute in the ith tube, F_{iv} is the axial volume flow in the ith tube, J_{ik} is the outward transmural flux per unit length of the kth solute from the ith tube, J_{iv} is the outward transmural volume flux (primarily water), $J_{ip,k}$ is the transmural flux of the kth solute from the ith to the pth tube, $J_{ip,v}$ is the transmural volume flux from the ith to the pth tube, c_{ik} is the concentration of the kth solute in the ith tube, P_i is hydrostatic pressure, R_{iF} is flow resistance, and x is normalized distance along the axis, $0 \leq x \leq 1$.

Transmural fluxes are given by

$$J_{ip,k} = J_{ip,v}(1 - \sigma_{ip,k})(c_{ik} + c_{pk})/2 + h_{ip,k}(c_{ik} - c_{pk}) + \mathfrak{I}_{ip,k} \text{ and} \quad [7]$$

$$J_{ip,v} = h_{ip,v}[\Sigma_k RT(c_{pk} - c_{ik})\sigma_{ip,k} + P_i - P_p], \quad [8]$$

where $\sigma_{ip,k}$ is the Staverman reflection coefficient of the membrane separating the ith from the pth tube for the kth solute, $h_{ip,k}$ is its passive permeability for the kth solute, $h_{ip,v}$ is its hydraulic permeability coefficient, $\mathfrak{I}_{ip,k}$ is the metabolically driven transport from the ith to the pth tube, R is the gas constant, and T is the absolute temperature.

We assume that the metabolically driven transport obeys approximate Michaelis–Menten kinetics, i.e.

$$\mathfrak{I}_{ip,k} = a_{ip,k}/[1 + b_{ip,k}/c_{ik}], \quad [9]$$

where $a_{ip,k}$ is the maximum rate of transport and $b_{ip,k}$ is the Michaelis constant. All of the membrane parameters may be

functions of distance along the tube, but are assumed not to depend on concentrations, flows, or pressures. For any particular membrane some of them usually equal zero; e.g., for no active transport, $a_{ip,k} = 0$.

Boundary conditions for the above system of equations are that entering concentrations, pressures, and flows are specified at $x = 0$ (the corticomedullary border) for tubes corresponding to DHL and descending vasa recta (DVR). Concentrations, pressures and flows, entering AHL at $x = 1$ (the papilla) must match those leaving DHL. Similarly ascending vasa recta (AVR) must match DVR at $x = 1$. When vasa recta are approximated by the core we have the subsidiary equations

$$c_{4k}(1) = J_{4k}(1)/J_{4v}(1). \quad [10]$$

(We follow the general subscripting convention DHL = 1, AHL = 2, CD = 3, core or AVR = 4, DVR = 5, and DN = 6.) When distal cortical nephron§ (DN) is included in the model, it is assumed to exchange with an external bath of fixed composition and pressure; distance varies from 0 to 1 along the DN, entering concentrations, flows, and pressures must match those for AHL at $x = 0$, and final values for DN at $x = 1$ must match entering values for CD at $x = 0$. When DN is not included, then entering concentrations, flows, and pressures for CD are specified.

To approximate the differential Eqs. **1** and **2** by difference equations, the medulla (and distal tubule) were divided into N segments and the difference equations

$$F_{ik}(j+1) - F_{ik}(j) = -[J_{ik}(j+1) + J_{ik}(j)]/(2N), \quad [11]$$

$$F_{iv}(j+1) - F_{iv}(j) = -[J_{iv}(j+1) + J_{iv}(j)]/(2N), \quad [12]$$

and

$$P_i(j+1) - P_i(j) = -R_{iF}[F_{iv}(j+1) + F_{iv}(j)]/(2N), \quad [13]$$

were written for each segment, where $F_{ik}(j)$ is the flow of the kth solute at $x = j/N$. If R_{iF} is very small, pressure is nearly constant throughout the system and drops out of the equations. The system of Eqs. **11** and **12** can then be solved iteratively as follows.

The functions

$$\phi_{ijk} = -F_{ik}(j+1) + F_{ik}(j) - [J_{ik}(j+1) + J_{ik}(j)]/(2N) \quad [14]$$

are defined. An initial estimate is then made of the $c_{ik}(j)$. From Eqs. **12** and **8** and the boundary conditions, the $F_{iv}(j)$ are then computed. It can be seen that these are functions only of the $c_{ik}(j)$ and the hydraulic permeabilities. Then substituting these $F_{iv}(j)$ into Eq. **5**, the resulting $F_{ik}(j)$ into Eq. **11** and using Eqs. **7** and **9** gives the ϕ_{ijk} as functions of the $c_{ik}(j)$ only. The deviation of each ϕ_{ijk} from 0 is a measure of the rate (positive or negative) at which the kth solute is accumulating in the jth segment of the ith tube for the particular initial choice of the $c_{ik}(j)$.

For a steady state solution we require $|\phi_{ijk}| < \epsilon$ for all i, j, and k, where ϵ is some preset tolerance. Ordinarily the tolerance condition is not satisfied by the initial choice of the $c_{ik}(j)$. To improve the estimate, the Jacobian matrix, G, of the partial derivatives $\partial\phi_{ijk}/\partial c_{qr}(s)$ is computed numerically.

§ In our terminology distal cortical nephron includes the cortical portion of thick AHL, distal convoluted tubule, and cortical collecting duct.

The system of linear equations

$$\phi - G\Delta c = 0, \quad [15]$$

where ϕ is the vector of the accumulation functions ϕ_{ijk} and c the vector of the $c_{ik}(j)$, is then solved by Gaussian elimination and back substitution to give the correction $\Delta c = G^{-1}\phi$ to the vector of concentrations. If G is singular, which occurs occasionally, an approximation to the Moore–Penrose generalized inverse of G is then substituted for G^{-1}. The approximation is $G^+ \simeq (G^TG + \tau I)^{-1}G^T$, where G^+ is the generalized inverse, G^T is the transpose of G, and τ is a small positive number (7, 8). The next approximation of the concentration vector $\hat{c}$ is given by

$$\hat{c} = c - t\Delta c, \quad [16]$$

where t is a scalar chosen to maximize convergence to the solution $\max_{i,j,k} |\phi_{ijk}| < \epsilon$. ($t = 1$ corresponds to the Newton–Raphson method and is ordinarily used.)

The method is both efficient and stable. For $\epsilon = 10^{-6}$ and initial entering total solute flow in DHL equal approximately to 1, four to ten iterations are usually needed to obtain a solution. The number of iterations depends primarily on the initial estimate and is relatively independent of the number of functions ϕ_{ijk}. The time per iteration increases roughly as the cube of the total number of equations (Eq. **14**). In most of the computations given below the number of spatial segments for each tube is 10; thus, the total number of equations varies from 20 for a single-solute, two-tube (core and DHL) model to 120 for a two-solute, six-tube (DHL, AHL, CD, DN, AVR, and DVR) model. Correspondingly, the time per iteration ranged from a fraction of a second to about 5 sec on an IBM 370/165. A suitable number of spatial divisions was empirically determined. From experimentation with 5, 10, 20, and 40 divisions with the simpler models, and 5, 10, and 20 chops with the more complex models, and comparison with values obtained by "shooting" methods (5), we found 10 spatial divisions to give concentrations within 5% of limiting values for most problems. As yet we have no rigorous estimates of how closely solutions of the difference equations approximate exact solutions of the differential equations in two-solute models with discontinuous transmembrane fluxes. The tolerance ϵ for solute accumulation is critical: $\epsilon = 10^{-2}$ can give grossly inaccurate results (it can be seen that for a total of 50 spatial segments this tolerance can permit a total solute accumulation of 50% entering DHL solute flow); $10^{-2} > \epsilon > 10^{-3}$ can give errors of several percent, $\epsilon = 10^{-3}$ one or two percent; and from $\epsilon = 10^{-4}$ to $\epsilon = 10^{-5}$ there is usually no significant change in the c vector. Usually the maximum residual in the ϕ_{ijk} functions decreases by an order of magnitude per iteration and can be taken to $\epsilon < 10^{-13}$, the limit set by machine roundoff error. In the results given in this paper, $\epsilon = 10^{-6}$ was taken as the criterion for a solution.

Central core model as a limiting case

For a single solute and a water extracting mode of operation, the central core model reduces to the prototype two-tube model shown in Fig. 1. If the hydraulic coefficient of the membrane separating core and DHL is large enough so that concentrations in core and DHL are nearly equal, then central core theory (2) predicts that the concentration ratio of papilla to cortex will approach

$$r = 1/(1 - f), \quad [17]$$

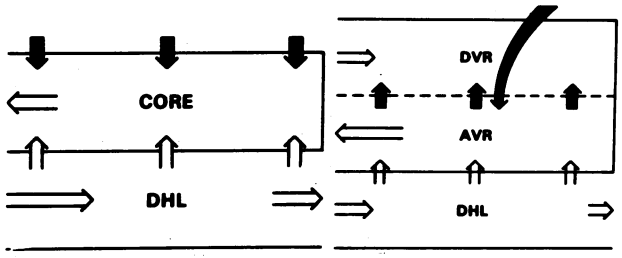

FIG. 1 (*left*). Prototype two-tube model.
FIG. 3 (*right*). Coupled DHL-vasa recta model. The core of the two-tube model has been replaced by a vascular exchanger.

where f is the fraction of entering descending limb solute flow supplied to the core; thus, if $f = 0.9$, $r = 10$. For finite permeabilities, core concentration will exceed DHL concentration. As a result, fluid leaving the core will be slightly hypertonic, less water will be extracted from DHL, and the concentration ratio will decrease. In Fig. 2 the concentration profiles in DHL, as computed by the method described above, are plotted for different normalized values of the hydraulic permeability. The easiest way to grasp the physiological significance of h_v is to note that for $h_v = 100$, the driving force for water movement, for a total osmolality of 300 mOsm for entering DHL fluid, would vary from 13 mOsm at the corticomedullary junction to 0.38 mOsm at the papilla. Stated in conventional units we find that for an DHL flow of 6 nl/min at the corticomedullary junction, a DHL diameter of 20 μm, and a total medullary depth of 1 cm, this would correspond to an osmotic coefficient $L_p \simeq 2 \times 10^{-4}$ ml·cm^{-2}·sec^{-1}·atm^{-1}. This is to be compared with a measured value of 1.62×10^{-4} ml·cm^{-2}·sec^{-1}·atm^{-1} in isolated rabbit DHL (9).

The concentrating ability of the medulla is critically dependent on the exchange efficiency of the vasa recta. As this becomes large the concentration ratio approaches the limit set by the permeability of Henle's limb. This point is illustrated in Figs. 3 and 4. In the model illustrated in Fig. 3, the core of the model in Fig. 1 is replaced by a vascular exchanger. In Fig. 4, concentration profiles for this model are plotted for increasing values of h_s, the normalized solute permeability of the membrane separating AVR and DVR. In this computation, entering DVR flow was assumed to be 10 times entering DHL flow. Thus, if DVR exchanged isotope with an outside bath at zero isotope concentration, concentration in DVR would decay as $\exp(-h_s x/10)$. It can be seen from Fig. 4, that as h_s increases, the concentration approaches the limit set by the central core model, but that the closeness of approach is critically dependent on h_s. It can be shown (10) that if the hydraulic permeability is such that DHL concentration approximately equals DVR concentration and DVR volume flow is much greater than DHL volume flow, then the concentration ratio for the system is given by

$$r = 1/[1 - f_T(1 - f_U)(1 - f_W)], \qquad [18]$$

where r is the concentration ratio, f_T is fractional solute transport out of AHL, f_U is the ratio of CD flow to combined CD and DHL flow at the papilla, and f_W measures the effect of vascular washout. Essentially it is the fraction of solute that leaves the system unaccompanied by its isotonic equivalent of

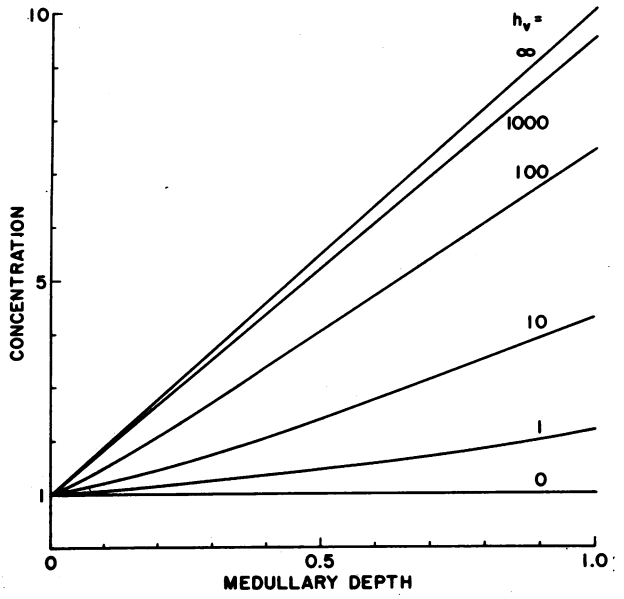

FIG. 2. Concentration profiles of DHL of prototype model for different hydraulic permeabilities of DHL.

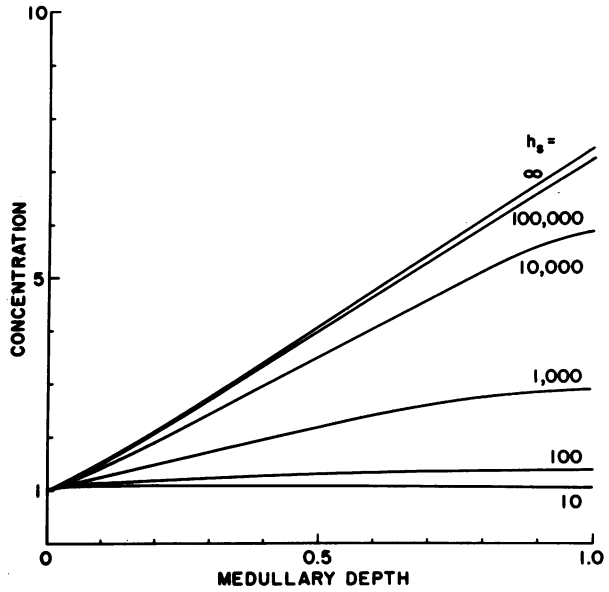

FIG. 4. Concentration profiles in coupled three-tube model as a function of vasa recta solute permeability. Normalized water permeability h_v of DHL was 100 in these computations.

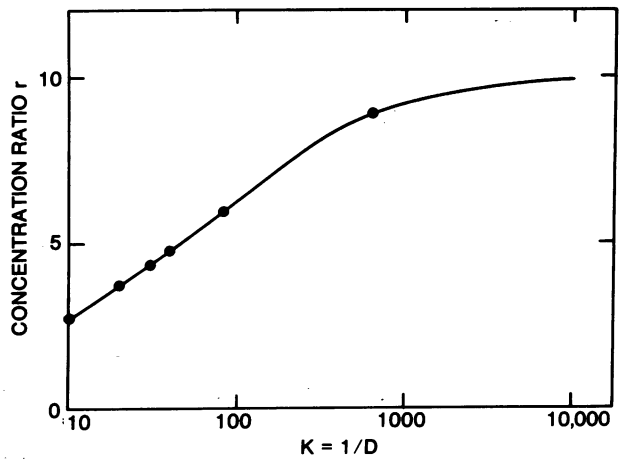

FIG. 5. Concentration ratio of three-tube model as a function of exchange efficiency K, for both the approximate analytic solution (——) and the numerical solutions (●).

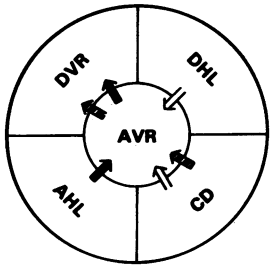

FIG. 6. Medullary cross-sectional configuration of six-tube, two-solute model. AHL and CD are connected by DN (not shown). Water movement is indicated by *white arrow*, salt movement by *black arrow*, and urea movement by *striped arrow*. Permeabilities are as implied by the transmural fluxes; e.g., DHL is impermeable to salt and urea. In the outer medulla, $0 \leq x \leq 0.5$, salt transport out of AHL is active; in the inner medulla, $0.5 \leq x \leq 1.0$, passive.

water. It can also be shown that

$$f_W \simeq [1 - \exp(-1/(Dr))](Dr), \qquad [19]$$

where $D \equiv (F_{dv})^2/h_s$ is an effective diffusion coefficient for the vascular exchanger, and F_{dv} is volume flow in the vasa recta. If f_W from Eq. **19** is substituted into Eq. **18** one obtains a transcendental equation in r. In Fig. 5, r as determined by Eqs. **18** and **19** is plotted as a function of $K \equiv 1/D$ for $f_T(1 - f_U) = 0.9$ and is compared with values obtained from numerical solution of the differential equations. As can be seen, agreement is excellent.

Passive function of the inner medulla

A major theoretical result of the central core model was that the medullary counterflow system was capable of concentrating by the passive mixing of salt and urea in the inner medulla, with no active salt transport out of the thin AHL, provided that salt, urea, and water permeabilities together with entering flows and concentrations were suitable (1, 3). Kokko and Rector independently proposed a qualitative model in which salt movement out of thin AHL is passive and secondary to urea diffusion into the inner medulla from CD (11). With the mathematical method described above it has been possible to analyze the role of salt and urea mixing in concentration in models that include AHL, DHL, CD, DN, AVR, and DVR. In the medulla the cross-sectional configuration of the system is as shown in Fig. 6, with solute and water exchange as indicated. In Figs. 7 and 8, concentration profiles are shown for active salt transport restricted to the outer medulla ($0 \leq x \leq 0.5$) and equal to 0.9 of entering DHL load. Salt concentration was taken as 1.0 and urea as 0.05 in entering DHL and DVR flow, i.e., 300 m0sm and 15 m0sm. In Fig. 7 is shown the effect of varying urea permeability of CD for fixed salt permeability of AHL and in Fig. 8 the effect of varying salt permeability of thin AHL for fixed urea permeability of CD. These computations have borne out the predictions of the idealized central core theory—namely, that the inner medulla ($0.5 \leq x \leq 1$) can develop a concentration gradient with no active transport, but that for it to do so, thin AHL must be highly permeable to salt; e.g. with the same conversion factors as for h_v, $h_{2s} = 10$ corresponds to a salt permeability of 16×10^{-5} cm·sec^{-1}.

Power utilization in the medulla

The rates of free energy change due to various processes going on in the renal medulla are related (12) by the general balance equation

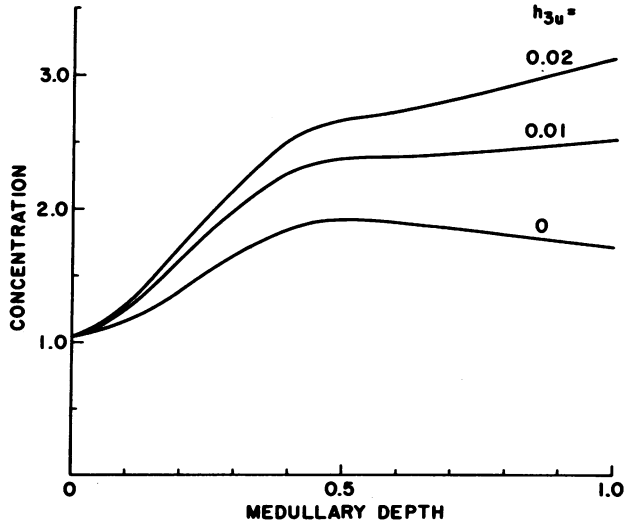

FIG. 7. Passive concentration in the inner medulla. Effect on total concentration in DHL of varying urea permeability h_{3u} of CD with salt permeability of thin AHL fixed at $h_{2s} = 10$ in normalized units.

$$RT\{\Sigma_k\Sigma_i[(F_{ik} \ln c_{ik})_{x=1} - (F_{ik} \ln c_{ik})_{x=0}]\}$$
$$= RT\Sigma_k\left\{\int_0^1 \sum_{\substack{i,p \\ i>p}} [-J_{ip,k} \ln (c_{ik}/c_{pk}) + J_{ip,v}(c_{ik} - c_{pk})]dx - \int_0^1 \Sigma_i \frac{D_{ik}A_i}{c_{ik}}\left(\frac{dc_{ik}}{dx}\right)^2 dx\right\}, \qquad [20]$$

where D_{ik} is the diffusion coefficient of the ith solute in the kth tube, and A_i is the cross-sectional area of the ith tube. Substituting from the phenomenological Eqs. **7** and **8** for transmural fluxes into Eq. **20**, assuming $D_{ik} \simeq 0$ and $\sigma_{ip,k} \simeq 1$, and using the relation $F_{Uk} = (\Sigma_i F_{ik})_{x=1}$; where F_{Uk} is the CD outflow of the kth solute; we obtain

$$RT\Sigma_k\{F_{Uk} \ln (c_{Uk}/c_{ok}) - \Sigma_i [F_{ik} \ln (c_{ik}/c_{ok})]_{x=0}\}$$
$$= RT\left\{\Sigma_k \int_0^1 \sum_{\substack{i,p \\ i>p}} -[h_{ip,k}(c_{ik} - c_{pk}) + \mathfrak{J}_{ip,k}] \ln (c_{ik}/c_{pk})dx - \int_0^1 \sum_{\substack{i,p \\ i>p}} RTh_{ip,v}(c_{iM} - c_{pM})^2 dx\right\}, \qquad [21]$$

where c_{ok} is a reference concentration for the kth solute (usually one of the entering concentrations), c_{iM} is total solute concentration in the ith tube, and c_{UK} is concentration of the kth solute in CD outflow.

The left hand side of Eq. **21** is the rate at which free energy outflow from the medulla exceeds free energy inflow; the right hand side is the rate at which free energy is being created or destroyed by transport of solutes and water across the membranes separating the tubes. With the possible exception of active transport terms of the form $\mathfrak{J}_{ip,k} \ln (c_{ik}/c_{pk})$, all terms on the right hand side of Eq. **21** are negative and represent power dissipation in the membranes. Thus $-RT\int_0^1 h_{ip,k}(c_{ik} - c_{pk}) \ln (c_{ik}/c_{pk})dx$ is the rate of energy dissipation in the passive diffusion of the kth solute across the membrane separating the ith and pth tubes. In Table 1, we have computed relative power use for the case $h_{3u} = 0.02$, $h_{2s} = 10$, illustrated in Fig 7. Note that the power supplied to the system

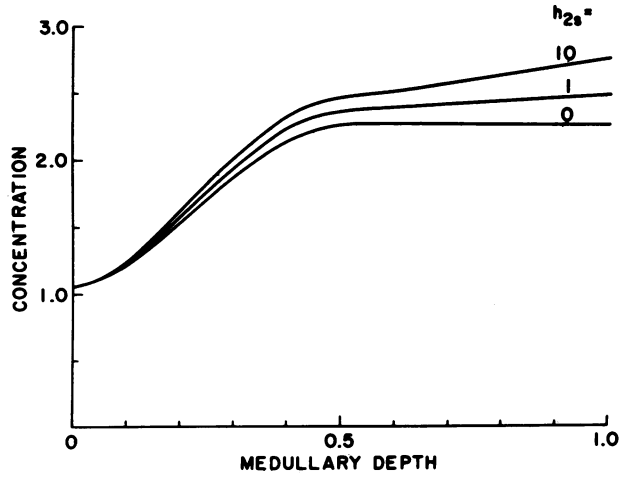

FIG. 8. Effect on total solute concentration in DHL of varying salt permeability h_{2s} of thin AHL with CD urea permeability h_{3u} fixed at 0.01 and with CD active urea source of strength .01 in normalized units. Note that for a positive concentration gradient to be developed in the inner medulla by passive transport, both $h_{2s} > 0$ and $h_{3u} > 0$ are required.

by the distal nephron is the difference between the rate of free energy outflow from AHL and free energy inflow via CD. The sum of the power supplied to the system by DN and thick AHL is normalized to 1. For this particular case, only 12% of this power is used to increase the free energy of solutes in the final urine. In the ideal central core models, the losses due to imperfect vascular exchange and finite hydraulic permeabilities of DHL and CD would disappear, but dissipation in the inner medulla from salt diffusion of thin AHL and urea diffusion out of CD would remain.

This type of calculation says nothing whatsoever about the efficiency with which metabolic energy is coupled to active salt transport, but does indicate the fraction of the energy supplied to the medulla by active salt transport that goes into increasing the free energy of solutes in the final urine.

TABLE 1. *Relative power use in the renal medulla**

Power supplied	
DN	0.201
AHL†	0.799
Total	1.000
Power used	
Solute loss vasa recta	0.376
Membrane dissipation	
CD urea	0.096
AHL salt‡	0.007
AVR salt	0.159
AVR urea	0.024
DHL water	0.207
CD water	0.004
Subtotal	0.497
Solute concentration in urine	
Salt§	—
Urea	0.119
Total¶	0.992

* Computations are for the case $h_{3u} = 0.02$ and $h_{2s} = 10$ shown in Fig. 7.

† Active transport integral for thick AHL.

‡ Passive diffusion integral for thin AHL.

§ Because of active salt transport out of AHL and DN a negligible amount is excreted in final urine for this case.

¶ The difference 0.008 between supply and use represents the cumulative error of the various integrations.

DISCUSSION

The results for single solute systems (Figs. 2, 4, and 5) show that concentration profiles of systems with finite permeabilities approach profiles for ideal central core models as permeabilities become large and confirm the hypothesis that central core concentrating engines are the prototype for the operation of the nephrovascular units of the renal medulla. The calculations on non-ideal two solute models (Figs. 7 and 8) have established that, like ideal central core systems, they can concentrate with no active transport in the inner medulla, but again only if they have very high salt permeabilities of thin AHL. The numerical solutions have also permitted an estimate of the range of permeabilities required for solute concentration in a given type of model. Finally, by combining the present quantitative kinetic analysis with earlier thermodynamic analysis (12), it has been possible for the first time to calculate in a given model the relative fractions of power used in increasing the free energy of solutes in the final urine and dissipated in frictional resistance to the transmembrane flow of solutes and water (Table 1).

The modified Newton–Raphson method used to obtain these numerical solutions is computationally efficient and stable, and is permitting for the first time quantitative comparison of both steady state and transient behavior¶ of a wide spectrum of models of the renal counterflow system. These first results show that a model can concentrate effectively only if its membrane permeabilities and other transport parameters fall within rather sharply defined limits.

1. Stephenson, J. L. (1972) *Kidney Int.* **2**, 85–94.
2. Stephenson, J. L. (1973) *Biophysical J.* **13**, 512–545.
3. Stephenson, J. L. (1973) *Biophysical J.* **13**, 546–567.
4. Kriz, W. (1970) in *Urea and the Kidney*, ed. Schmidt-Nielsen, B. (Excerpta Medica Foundation, Amsterdam), pp. 342–357.
5. Mejia, R. & Stephenson, J. L. (1973) Conference Proceedings. 1973 Summer Computer Simulation Conference (Simulation Councils, Inc., La Jolla), Vol. 2, pp. 806–810.
6. Stephenson, J. L. (1973) in *Engineering Principles in Physiology*, eds. Brown, J. H. U. & Gann, D. S. (Academic Press, New York and London), Vol. 2, pp. 283–320.
7. Ben-Israel, A. (1965) *Report AD 639-464* (Defense Documentation Center, Washington, D.C.).
8. Albert, A. & Sittler, R. W. (1965) *SIAM J. on Control* **3**, 1–31.
9. Kokko, J. P. (1970) *J. Clin. Invest.* **49**, 1838–1846.
10. Stephenson, J. L. (1973) *Biophys. Soc. Abstr.* **13**, 133a.
11. Kokko, J. P. & Rector, F. C., Jr. (1972) *Kidney Int.* **2**, 214–223.
12. Stephenson, J. L. (1974) *Math. Biosci.*, in press.
13. Stephenson, J. L., Tewarson, R. P. & Mejia, R. (1973) in "Abstracts," *6th Annu. Meeting, Amer. Soc. Nephrol.*, p. 100.

¶ The method extends readily to transient problems, giving a fully implicit scheme for solving the finite difference approximation of the partial differential equations that appears to be unconditionally stable (unpublished).